ECS Journal of Solid State
Science and Technology

1 mm^2, 3.6 kV, 4.8 A NiO/Ga_2O_3 Heterojunction Rectifiers

To cite this article: Jian-Sian Li *et al* 2023 *ECS J. Solid State Sci. Technol.* **12** 085001

ECS Journal of Solid State Science and Technology, 2023 **12** 085001

1 mm^2, 3.6 kV, 4.8 A NiO/Ga_2O_3 Heterojunction Rectifiers

Jian-Sian Li,[1] Chao-Ching Chiang,[1] Xinyi Xia,[1] Hsiao-Hsuan Wan,[1] Fan Ren,[1] and S. J. Pearton[2,z]

[1]*Department of Chemical Engineering, University of Florida, Gainesville, FL 32606 United States of America*
[2]*Department of Materials Science and Engineering, University of Florida, Gainesville, FL 32606 United States of America*

Large area (1 mm^2) vertical NiO/β n-Ga_2O/n^+ Ga_2O_3 heterojunction rectifiers are demonstrated with simultaneous high breakdown voltage and large conducting currents. The devices showed breakdown voltages (V_B) of 3.6 kV for a drift layer doping of 8×10^{15} cm^{-3}, with 4.8 A forward current. This performance is higher than the unipolar 1D limit for GaN, showing the promise of β-Ga_2O_3 for future generations of high-power rectification devices. The breakdown voltage was a strong function of drift region carrier concentration, with V_B dropping to 1.76 kV for epi layer doping of 2×10^{16} cm^{-3}. The power figure-of-merit, V_B^2/R_{ON}, was 8.64 GW·cm^{-2}, where R_{ON} is the on-state resistance (1.5 mΩ cm^2). The on-off ratio switching from 12 to 0 V was 2.8×10^{13}, while it was 2×10^{12} switching from 100 V. The turn-on voltage was 1.8 V. The reverse recovery time was 42 ns, with a reverse recovery current of 34 mA.
 [DOI: 10.1149/2162-8777/aceaa8]

Manuscript submitted May 16, 2023; revised manuscript received June 22, 2023. Published August 2, 2023. *This paper is part of the JSS Focus Issue on Sustainable Materials and Devices.*

There is great current interest in the development of power electronic devices based on monoclinic β-Ga_2O_3.[1–16] There have been demonstrations of high breakdown voltages above 8 kV in relatively small devices of both vertical rectifiers[8] and lateral transistors intended for lower current applications.[11–13] A promising recent development has been the use of NiO as a p-type conducting layer to produce p-n heterojunctions with the n-type Ga_2O_3.[17–31] This to some extent mitigates the lack of a native p-type doping capability for Ga_2O_3. There remain many challenges, including optimizing edge termination, and managing heat dissipation, which will be needed if adequate device reliability is to be achieved.[1,3,23,32–38] Another crucial focus is to have larger area devices to achieve high conduction currents, while simultaneously retaining the kV breakdown characteristics.[23,32,34–43] Qin et al.[1] recently reviewed the status of packaging and device performance of Ampere-class Ga_2O_3 Schottky, Junction Barrier Schottky, hetero-junction rectifiers and MOSFETs and their switching recovery characteristics, and surge-current and over-voltage ruggedness.

While small area devices now have breakdown voltages exceeding the unipolar limit of both SiC and GaN power devices, large area, Ampere-class Ga_2O_3 vertical devices have not yet reached this milestone.[1]

In this paper, we demonstrate 1 mm^2, 4.8 A, 3.6 kV V_B vertical NiO/Ga_2O_3 rectifiers, with performance above the unipolar limit of both GaN and SiC. The power figure of merit (FOM) is 8.64 GW.cm^{-2}, with reverse recovery time of 42 ns.

Experimental

Figure 1 top shows a schematic of the vertical heterojunction rectifier structure. The drift region was a 10 μm thick, lightly Si doped (8×10^{15} cm^{-3}) layer grown by halide vapor phase epitaxy (HVPE) on a (001) surface orientation Sn-doped β-Ga_2O_3 single crystal (Novel Crystal Technology, Japan). The X-ray diffraction full width at half maximum of the substrates are <350 arc.s in both [100] and [010] directions. For comparison, we also fabricated devices in the identical fashion on structures with drift region doping 2×10^{16} cm^{-3}, also obtained from Novel Crystal Technology. The backside Ohmic contact used e-beam evaporated Ti/Au with a total thickness of 100 nm. This was annealed at 550 °C for 60 s under N_2.[10,32,33] The p-n heterojunction was formed by rf magnetron sputter deposition of a bilayer of NiO.[10] The working pressure was 3mTorr at 80 W power. The deposition rate of 0.06 Å.s^{-1}. This is very slow but is necessary to avoid damage to the Ga_2O_3 surface. The bias voltage on the cathode of the sputtering system is around 50 V at 80 W power. At higher biases, we have noted visible lattice disorder by electron microscopy.[10] Full details of the properties of the NiO have been published elsewhere.[44] Contact to the NiO was made through e-beam deposition of 100 nm total thickness of Ni/Au with contact diameter 1 mm. An optical image of the completed devices is shown in Fig. 1(bottom).

Current-voltage (I-V) characteristics were recorded in Fluorinert atmospheres at 25 °C on a Tektronix 371-B curve tracer and Glassman high voltage power supply. An Agilent 4156 C was also used for forward and reverse current characteristics. The reverse breakdown voltage was obtained from the standard definition of reverse current reaching 1 mA.cm^2. The on-resistance was calculated from the slope dV/dI of the I-V characteristics[8,26] and corrected for the resistance of the external circuit (cables, chuck and probe), which was 10 Ω. The on-resistance values were calculated assuming the current spreading length is 10 um and a 45° spreading angle. The R_{ON} normally reported is the unipolar drift resistance, which is usually smaller than the diffusion resistance. The I-V characteristics were reproducible over areas of 1 cm^2 on the wafer, with absolute currents within 20% at a given voltage.

Results and Discussion

The forward I-V characteristics are shown in Fig. 2 (a) for the 1 mm diameter devices fabricated with the 8×10^{15} cm^{-3}drift layers. The maximum forward current was 4.8 A, with 1 A reached at 4 V forward. This shows the presence of the p-n junction does not prevent reaching high forward currents at moderate biases. The on-resistance was 1.5 mΩ. cm^{-2}. The on-off ratio was 2×10^{13} for switching from 12 V to 0 V. The same data is shown in linear form in Fig. 2 (bottom), showing the turn-on voltage was 1.8 V.

The reverse I-V characteristics are shown in Fig. 3 (top) for the devices fabricated on both the 8×10^{15} cm^{-3} and 2×10^{16} cm^{-3} drift layers. The former exhibit breakdown voltage (V_B) values of 3.6 kV, the highest yet reported for large area Ga_2O_3 rectifiers.[1] The decrease in drift layer carrier concentration has a significant effect on V_B, with the devices with higher doping having breakdown voltages roughly half that of the lower doped devices. The power figure of merit was 8.64 GW.cm^{-2} for the 3.6 kV devices. This is approximately 25% of the theoretical maximum for β-Ga_2O_3, showing there is still room for optimizing device design and material defect density.[1–5] The average electric field strength was 3.56 MV cm^{-1},

[z]E-mail: spear@mse.ufl.edu

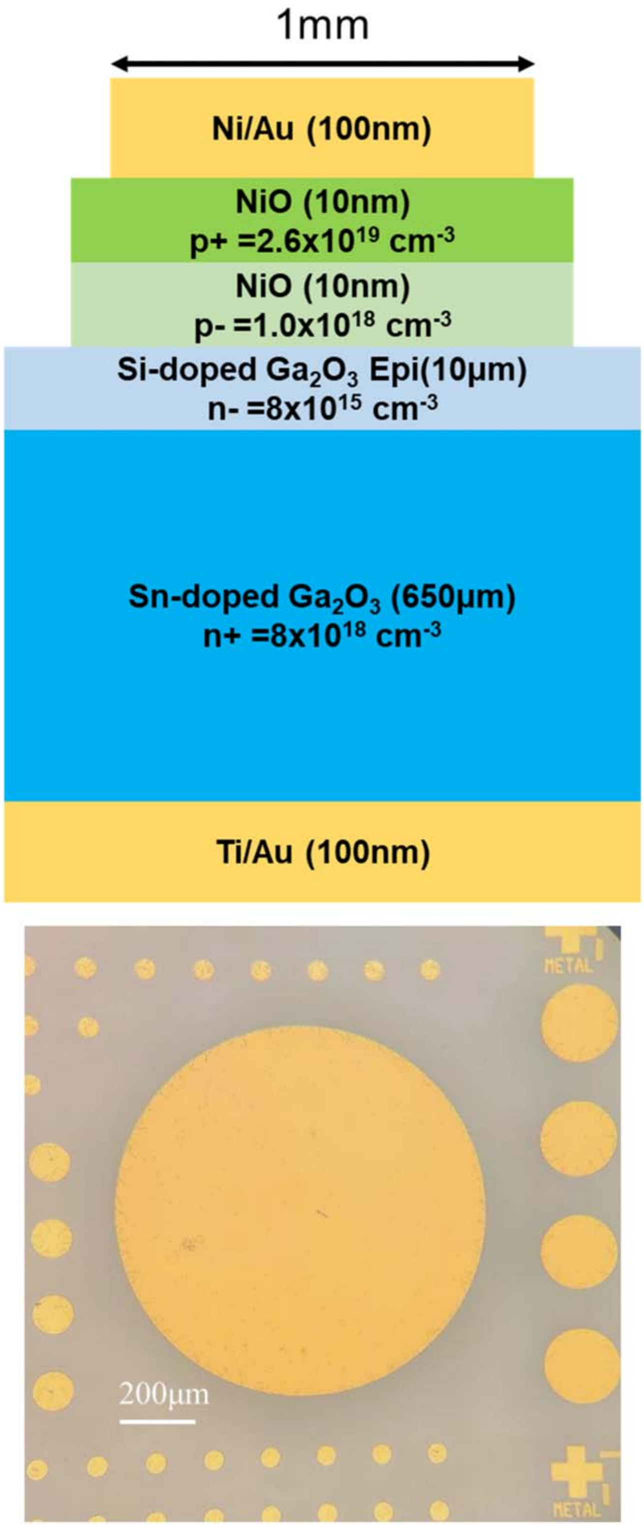

Figure 1. (top) Schematic of NiO/Ga_2O_3 heterojunction rectifier. (bottom) optical micrograph of array of 1 mm^2 rectifiers.

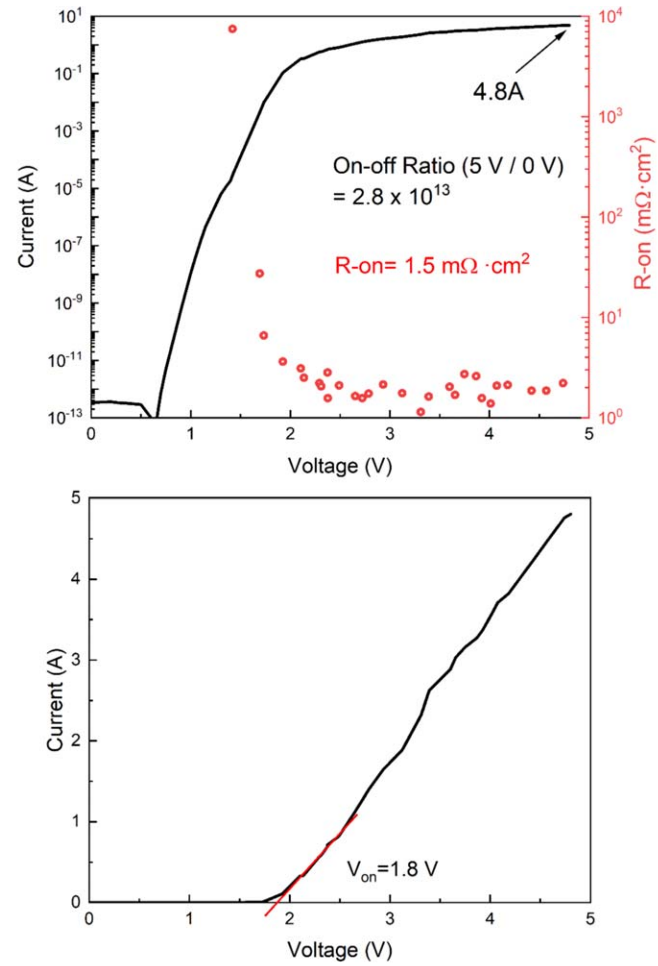

Figure 2. (top) Log plot of forward current densities and R_{ON} values of NiO/Ga_2O_3 heterojunction rectifiers (bottom) linear plot of forward I-V characteristics of NiO/Ga_2O_3 heterojunction rectifiers.

an appreciable fraction of the expected maximum near 8 $MV.cm^{-1}$ and among the highest reported, particularly for large area devices.[1,2] The bottom of Fig. 3 shows the reverse I-V up to −100V, with the current density being $<10^{-10}$ $A.cm^{-2}$ to this voltage. As previously reported, there are several leakage current mechanisms present, including variable range hopping and trap-assisted space-charge-limited current.[10,20,30] The former shows a linear relationship of ln(J)-E at lower biases, while at higher voltages, there is a linear relationship of ln (J)-ln (*V*).

The on/off ratio when switching from 12 V forward to the reverse bias on the *x*-axis is shown in Fig. 4 for the 1 mm^2 devices with the low drift layer concentration. The values are $>2 \times 10^{12}$ when switching to −100V, showing the excellent rectification characteristics of these large area devices and the highest yet reported.[1]

Figure 5 shows the reverse recovery waveform when switching from 120 mA forward current at a duty cycle of 2%. The reverse recovery time is 42 ns, with a reverse recovery current of 34 mA. The recovery time is approximately twice that for small rectifiers with areas 5–8 $\times$ 10^{-3} mm^2, i.e. 100–200 x smaller than the 1 mm^2 devices.[10,45,46]

To place the work in context, Fig. 6 shows a compilation of reported Ron vs V_B results reported in the literature for Ampere-class rectifiers and includes conventional Schottky barrier or JBS rectifiers and NiO/Ga_2O_3 heterojunction rectifiers.[23,33–44] The theoretical lines for the 1D unipolar limits of SiC, GaN and Ga_2O_3 are also shown. The result in this work is the first demonstration of large area, Ampere-class Ga_2O_3 rectifiers surpassing the theoretical limits of GaN and SiC.

Figure. 7 shows a compilation of on/off ratios as a function of the Baliga FOM for large area Ga_2O_3 rectifiers. The results in this current work show how lowering the drift region carrier concentration and optimization of the device processing parameters have led to improvement in device performance. For example, the reduction in carrier density made a more than 2x improvement in V_B, while

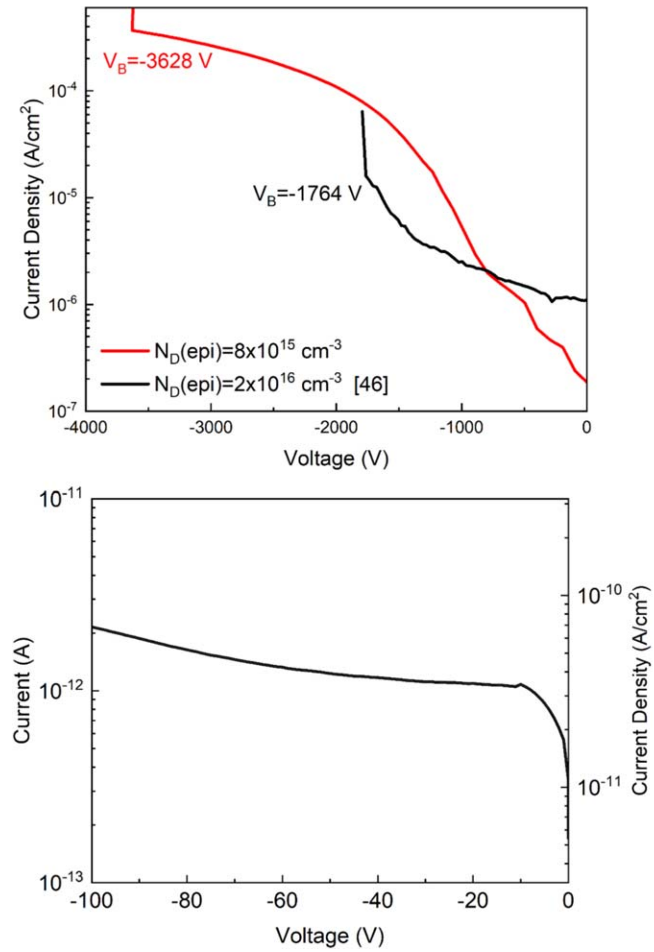

Figure 3. (top) Reverse I-V characteristics and breakdown voltage of NiO/Ga_2O_3 heterojunction rectifiers. (bottom) expanded view of reverse leakage current-bias voltage characteristics to −100V.

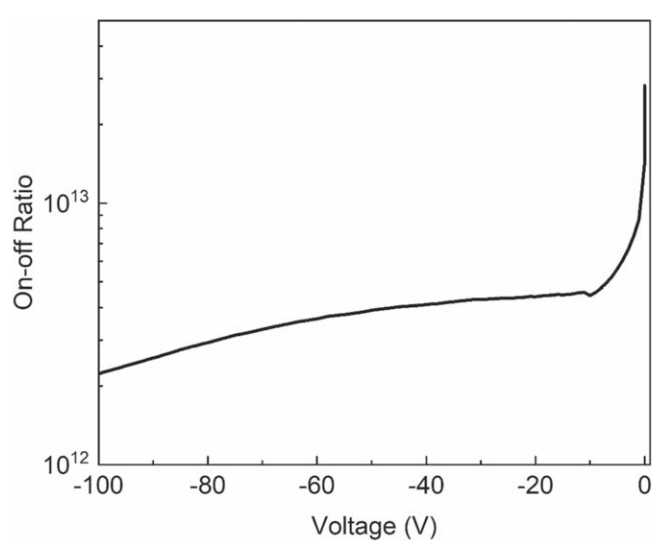

Figure 4. On-off ratio of NiO/Ga_2O_3 heterojunction rectifiers in which the bias was switched from 5 V forward to the voltage shown on the *x*-axis.

optimizing the NiO thickness and doping also had significant effects on the dc characteristics.

We have recently examined the high temperature performance of NiO/Ga_2O_3 rectifiers and found them to be much more stable up to

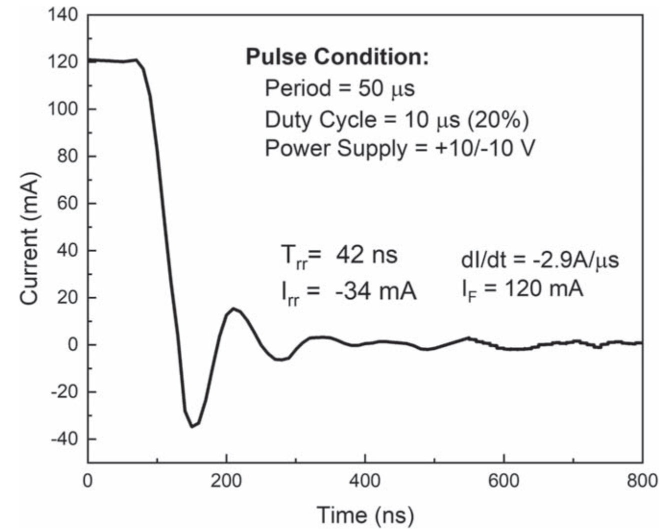

Figure 5. Switching waveform for NiO/Ga_2O_3 heterojunction rectifiers for a 2% duty cycle.

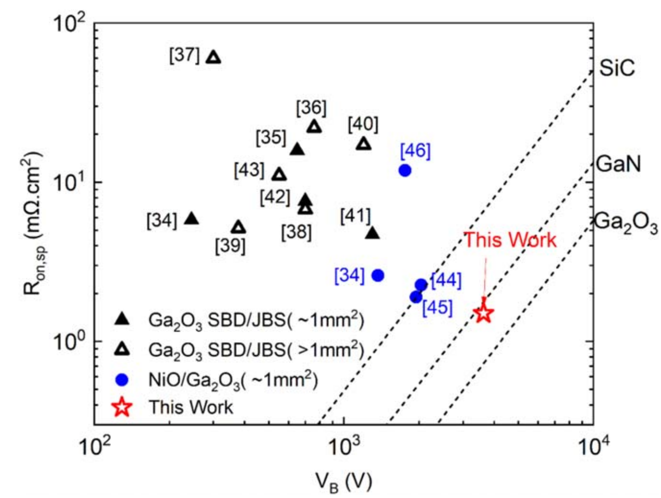

Figure 6. Compilation of Ron vs V_B of conventional and NiO/Ga_2O_3 heterojunction rectifiers reported in the literature.

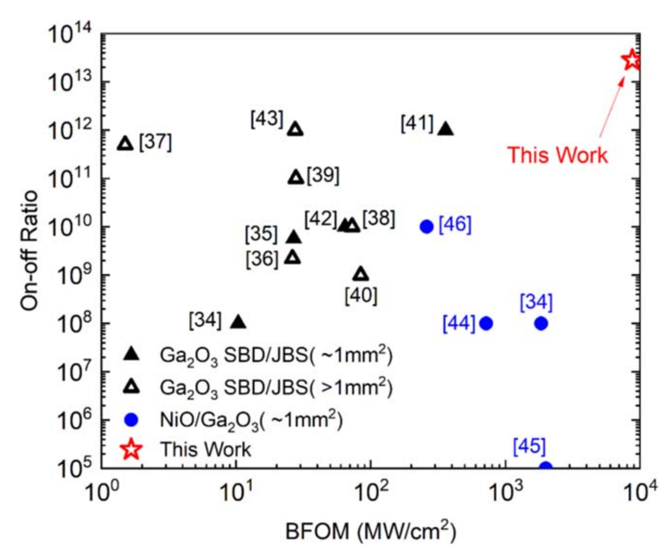

Figure 7. Compilation of on-off ratio vs BFOM of conventional and NiO/Ga_2O_3 heterojunction rectifiers reported in the literature.

600 K than Schottky rectifiers fabricated on the same wafers.[47,48] Such devices exhibit breakdown fields >8.5 MV.cm^{-1}, establishing this as a lower limit for β-Ga_2O_3.[49]

Summary and Conclusions

In summary, we report large area NiO/β-Ga_2O_3 p-n heterojunction rectifiers with V_B 3.6 kV, on/off ratio $>2 \times 10^{12}$ up to 100 V, with R_{on} of 1.5 mΩ·cm^2 and a figure-of-merit (V_b^2/R_{on}) of 8.64 GW.cm^{-2}. The results show that with state-of-the-art epitaxial structures, the use of the NiO p-layer to form a heterojunction with the Ga_2O_3, a simple, planar fabrication technology produces results exceeding the 1D unipolar performance of GaN and SiC. This is very encouraging considering the other advantages of Ga_2O_3, including low production costs and scalable bulk growth technology. A key area for future work is to reduce the damage created by sputtering of the NiO, perhaps by using direct MOCVD growth, as demonstrated recently.[50] There also needs to be further understanding of edge termination and possible minority carrier effects on modulation.[51–53]

Acknowledgments

The work at UF was performed as part of Interaction of Ionizing Radiation with Matter University Research Alliance (IIRM-URA), sponsored by the Department of the Defense, Defense Threat Reduction Agency under award HDTRA1–20–2–0002. The content of the information does not necessarily reflect the position or the policy of the federal government, and no official endorsement should be inferred. The work at UF was also supported by NSF DMR 1856662.

Data availability

The data that supports the findings of this study are available within the article l.

Declarations

The authors have no conflicts to disclose.

ORCID

Jian-Sian Li https://orcid.org/0000-0002-2817-7612
Chao-Ching Chiang https://orcid.org/0000-0002-0447-8170
Xinyi Xia https://orcid.org/0000-0002-8644-8599
Hsiao-Hsuan Wan https://orcid.org/0000-0002-6986-8217
S.J. Pearton https://orcid.org/0000-0001-6498-1256

References

1. Y. Qin et al., *J. Appl. Phys.*, **62**, SF0801 (2023).
2. M. H. Wong and M. Higashiwaki, *M., IEEE Trans Electron Dev*, **67**, 3925 (2020).
3. M. H. Wong, "High Breakdown Voltage β-Ga_2O_3 Schottky Diodes." *In Ultrawide Bandgap β-Ga_2O_3 Semiconductor: Theory and Applications* (AIP Publishing, Melville, NY) (2023).
4. A. J. Green et al., *APL Mater.*, **10**, 029201 (2022).
5. S. J. Pearton, F. Ren, M. Tadjer, and J. Kim, *J. Appl. Phys.*, **124**, 220901 (2018).
6. C. Wang, J. Zhang, S. Xu, C. Zhang, Q. Feng, Y. Zhang, J. Ning, S. Zhao, H. Zhou, and Y. Hao, *J. Physics D: Applied Physics*, **54**, 243001 (2021).
7. S. Sharma, K. Zeng, S. Saha, and U. Singisetti, *IEEE Electron Dev. Lett.*, **41**, 836 (2020).
8. J. Zhang et al., *Nature Comm.*, **13**, 3900 (2022).
9. P. Dong, J. Zhang, Q. Yan, Z. Liu, P. Ma, H. Zhou, and Y. Hao, *IEEE Electron Dev Lett*, **43**, 765 (2022).
10. J. S. Li, C. C. Chiang, X. Xia, T. J. Yoo, F. Ren, H. Kim, and S. J. Pearton, *Appl. Phys. Lett.*, **121**, 042105 (2022).
11. S. Roy, A. Bhattacharyya, P. Ranga, H. Splawn, J. Leach, and S. Krishnamoorthy, *IEEE Electron Dev Lett*, **42**, 1140 (2021).
12. A. Bhattacharyya, S. Sharma, F. Alema, P. Ranga, S. Roy, C. Peterson, G. Seryogin, A. Osinsky, U. Singisetti, and S. Krishnamoorthy, *Appl. Phys. Express*, **15**, 061001 (2022).
13. K. D. Chabak et al., *Semicond. Sci. Technol,*, **35**, 013002 (2019).
14. Z. Hu et al., *Appl. Phys. Lett.*, **113**, 122103 (2018).
15. R. Sharma, M. Xian, C. Fares, M. E. Law, M. Tadjer, K. D. Hobart, F. Ren, and S. J. Pearton, *J. Vac. Sci. Technol.*, **A39**, 013406 (2021).
16. W. Li, D. Saraswat, Y. Long, K. Nomoto, D. Jena, and H. G. Xing, *Appl. Phys. Lett.*, **116**, 192101 (2020).
17. Y. Lv et al., *IEEE Trans. Power Electron.*, **36**, 6179 (2020).
18. M. Xiao et al., *IEEE Trans Power Electron,*, **36**, 8565 (2021).
19. X. Lu, X. Zhou, H. Jiang, K. W. Ng, Z. Chen, Y. Pei, K. M. Lau, and G. Wang, *IEEE Electron Dev. Lett*, **41**, 449 (2020).
20. C. Wang et al., *IEEE Electron Dev. Lett.,*, **42**, 485 (2021).
21. Q. Yan et al., *Appl. Phys. Lett.*, **118**, 122102 (2021).
22. H. H. Gong, X. H. Chen, Y. Xu, F. F. Ren, S. L. Gu, and J. D. Ye, *Appl. Phys. Lett.*, **117**, 022104 (2020).
23. H. Gong et al., *IEEE Trans. Power Electron.*, **36**, 12213 (2021).
24. H. H. Gong et al., *Appl. Phys. Lett.*, **118**, 202102 (2021).
25. W. Hao, Q. He, K. Zhou, G. Xu, W. Xiong, X. Zhou, G. Jian, C. Chen, X. Zhao, and S. Long, *Appl. Phys. Lett.*, **118**, 043501 (2021).
26. F. Zhou et al., *IEEE Trans. Power Electron.*, **37**, 1223 (2021).
27. Q. Yan, H. Gong, H. Zhou, J. Zhang, J. Ye, Z. Liu, C. Wang, X. Zheng, R. Zhang, and Y. Hao, *Appl. Phys. Lett.*, **120**, 092106 (2022).
28. X. Xia, J. S. Li, C. C. Chiang, T. J. Yoo, F. Ren, J. Kim, and S. J. Pearton, *J. Phys. D: Appl. Phys.*, **55**, 385105 (2022).
29. J. Zhang, S. Han, M. Cui, X. Xu, W. Li, H. Xu, C. Jin, M. Gu, L. Chen, and K. H. Zhang, *ACS Appl. Electron. Mater.*, **2**, 456 (2020).
30. Y. Wang et al., *IEEE Trans. Power Electron.*, **37**, 3743 (2021).
31. H. Zhou, S. Zeng, J. Zhang, Z. Liu, Q. Feng, S. Xu, J. Zhang, and Y. Hao, *Crystals*, **11**, 1186 (2021).
32. J. Yang et al., *Appl. Phys. Lett.*, **114**, 232106 (2019).
33. J. Yang, F. Ren, F. Chen, Y. T. Liao, C. W. Chang, J. Lin, M. Tadjer, S. J. Pearton, and A. Kuramata, *IEEE J. Electron Dev. Soc*, **7**, 57 (2018).
34. J. Yang, F. Ren, M. Tadjer, S. J. Pearton, and A. Kuramata, *AIP Adv.*, **8**, 055026 (2018).
35. J. Yang, C. Fares, R. Elhassani, M. Xian, F. Ren, S. J. Pearton, M. Tadjer, and A. Kuramata, *ECS J. Solid State Sci. Technol.*, **8**, Q3159 (2019).
36. M. Ji, N. R. Taylor, I. I. Kravchenko, P. Joshi, T. Aytug, L. R. Cao, and M. P. Paranthaman, *IEEE Trans. Power Electron.*, **36**, 41 (2020).
37. M. Xiao et al., *IEEE Trans. Power Electron.*, **36**, 8565 (2021).
38. H. Gong, F. Zhou, X. Yu, X. Xu, F. F. Ren, S. Gu, H. Lu, J. Ye, and R. Zhang, *IEEE Electron Dev. Lett.*, **43**, 773 (2022).
39. F. Otsuka, H. Miyamoto, A. Takatsuka, S. Kunori, K. Sasaki, and A. Kuramata, *Appl. Phys. Express*, **15**, 016501 (2021).
40. W. Hao et al., "High-performance vertical β-Ga_2O_3 schottky barrier diodes featuring p-NiO JTE with adjustable conductivity." *In 2022 International Electron Devices Meeting (IEDM)*p. 9 (2022).
41. Y. Lv et al., *IEEE Trans. Power Electron.*, **3**, 6179 (2020).
42. J. Wei, Y. Wei, J. Lu, X. Peng, Z. Jiang, K. Yang, and X. Luo, "Experimental study on electrical characteristics of large-size vertical β-Ga_2O_3 junction barrier schottky diodes." *In IEEE 34th International Symposium on Power Semiconductor Devices and ICs (ISPSD)*p. 97.
43. F. Zhou et al., *Appl. Phys. Lett.*, **119**, 262103 (2021).
44. X. Jian-Sian Li, C.-C. Xia, D. C. Chiang, B. P. Hays, V. Gila, F. Craciun, S. J. Ren, J. V. Pearton, Sci, and A. Technol, *Journal of Vacuum Science & Technology A*, **41**, 013405 (2023).
45. J. S. Li, C. C. Chiang, X. Xia, C. T. Tsai, F. Ren, Y. T. Liao, and S. J. Pearton, *ECS J. Sol. State Sci. Technology*, **11**, 105003 (2022).
46. J. S. Li, C. C. Chiang, X. Xia, F. Ren, and S. J. Pearton, *J. Vac. Sci. Technol. A*, **40**, 063407 (2022).
47. J. S. Li, C. C. Chiang, X. Xia, H. H. Wan, F. Ren, and S. J. Pearton, *J. Mater. Chem. C*, **11**, 7750 (2023).
48. J. S. Li, H. H. Wan, C. C. Chiang, X. Xia, T. Yoo, H. Kim, F. Ren, and S. J. Pearton, *Crystals*, **13**, 886 (2023).
49. J. S. Li, C. C. Chiang, X. Xia, H. H. Wan, F. Ren, and S. J. Pearton, *J. Vac. Sci. Technol. A*, **41**, 043404 (2023).
50. A. S. Kondrateva, M. Mishin, A. Shakhmin, M. Baryshnikova, and S. E. Alexandrov, *Phys. Status Solidi C*, **12**, 912 (2015).
51. F. Zhou et al., *IEEE Trans. Power Electron., 37*, p. 1223 (2021).
52. W. Hao, Q. He, Z. Han, X. Zhao, G. Xu, S. Yang, and S. Long, "1 kV Vertical β-Ga_2O_3 heterojunction barrier schottky diode with hybrid unipolar and bipolar operation." *2023 35th International Symposium on Power Semiconductor Devices and ICs (ISPSD)*(Hong Kong)p. 394 (2023).
53. M. Xiao, B. Wang, R. Zhang, Q. Song, J. Spencer, Z. Du, Y. Qin, K. Sasaki, H. Wang, M. Tadjer, and Y. Zhang, "NiO junction termination extension for Ga_2O_3 devices: high blocking field, low capacitance, and fast switching speed." *2023 35th International Symposium on Power Semiconductor Devices and ICs (ISPSD)*, Hong Kong28 May–01 June 2023p. 386 (2023).